Development 136, 2049-2058 (2009) doi:10.1242/dev.033480

Inhibitory and excitatory subtypes of cochlear nucleus neurons are defined by distinct bHLH transcription factors, Ptf1a and Atoh1

Tomoyuki Fujiyama[1,2], Mayumi Yamada[1,2], Mami Terao[2], Toshio Terashima[3], Hiroyuki Hioki[4], Yukiko U. Inoue[1], Takayoshi Inoue[1], Norihisa Masuyama[1], Kunihiko Obata[5], Yuchio Yanagawa[6], Yoshiya Kawaguchi[7], Yo-ichi Nabeshima[2] and Mikio Hoshino[1,2,*]

The cochlear nucleus (CN), which consists of dorsal and ventral cochlear nuclei (DCN and VCN), plays pivotal roles in processing and relaying auditory information to the brain. Although it contains various types of neurons, the origins of the distinct subtypes and their developmental molecular machinery are still elusive. Here we reveal that two basic helix-loop-helix transcription factors play crucial roles in specifying neuron subtypes in the CN. Pancreatic transcription factor 1a (Ptf1a) and atonal homolog 1 (Atoh1) were found to be expressed in discrete dorsolateral regions of the embryonic neuroepithelia of the middle hindbrain (rhombomeres 2-5). Genetic lineage tracing using mice that express Cre recombinase from the *Ptf1a* locus or under the control of the *Atoh1* promoter revealed that inhibitory (GABAergic and glycinergic) or excitatory (glutamatergic) neurons of both DCN and VCN are derived from the Ptf1a- and Atoh1-expressing neuroepithelial regions, respectively. In the *Ptf1a* or *Atoh1* null embryos, production of inhibitory or excitatory neurons, respectively, was severely inhibited in the CN. These findings suggest that inhibitory and excitatory subtypes of CN neurons are defined by Ptf1a and Atoh1, respectively and, furthermore, provide important insights into understanding the machinery of neuron subtype specification in the dorsal hindbrain.

KEY WORDS: Hindbrain, Math1, bHLH transcription factor, Cochlear nucleus, Inhibitory, Excitatory, Mouse

INTRODUCTION

Sounds received in the ear are transmitted via the auditory nerve to the cochlear nucleus (CN) of the mammalian hindbrain, where the auditory information is properly processed and relayed to the brain. The CN is a very complex cell assembly, which can be divided into two subregions, the ventral and dorsal cochlear nuclei (VCN and DCN), that differ in structure and features.

Because of its importance in sound perception, the CN has been intensely studied from anatomical, physiological and histochemical points of view (Osen, 1969; Ryugo and Willard, 1985; Hackney et al., 1990). Histological observations have deduced that a portion of neurons generated from the dorsal hindbrain neuroepithelia migrate tangentially to give rise to CN neurons (Pierce, 1967; Ivanova and Yuasa, 1998). More directly, genetic-fate-mapping studies using transgenic mice confirmed that many CN cells are derived from the dorsal region of the hindbrain neuroepithelia, where the *Wnt1* promoter is active (Farago et al., 2006; Nichols and Bruce, 2006). As to the rostrocaudal axis, the origins of CN neurons seem to differ between avians and mammals. Grafting studies revealed that avian CN neurons are derived from a broader part of the hindbrain [rhombomeres (r) ~3-8] (Tan and Le Douarin, 1991; Cambronero and Puelles, 2000; Cramer et al., 2000), whereas mouse genetic studies have suggested a more rostral and narrower origin (~r2-5) (Farago et al., 2006).

Recently, Farago et al. (Farago et al., 2006) performed very sophisticated genetic-fate-mapping studies by using an FLP-FRT and Cre-loxP-based dual lineage-tracing system. In addition to showing that CN neurons are derived from ~r2-5, they also revealed that neurons in the anterior part of the VCN (aVCN), the posterior part of the VCN (pVCN) and the DCN are generated from rostral (~r2, 3), middle (~r3, 4) and caudal (~r4, 5) parts of the CN-neuron-producing hindbrain (~r2-5), respectively, although this tendency is not very strict and some overlap was observed.

The CN contains a variety of neurons that have distinct features (Osen, 1969; Ryugo and Willard, 1985; Hackney et al., 1990). For example, the DCN includes Golgi, molecular layer (ML)-stellate, cartwheel, tuberculo-ventral, unipolar brush, giant and fusiform cells, whereas the VCN is comprised of octopus, globular-bushy, spherical-bushy, T-stellate and D-stellate cells (Fig. 4A). Therefore, the CN is a good model system to investigate the molecular machinery underlying the specification of cell type identities. In other parts of the nervous system, such as the cerebellum and cerebral cortex, it is known that distinct subtypes of neurons are generated from distinct neuroepithelial regions (Wilson and Rubenstein, 2000; Ross et al., 2003; Hoshino, 2006). This implies that distinct subsets of neurons in the CN may be derived from discrete neuroepithelial origins. However, few fate-mapping studies have focused on CN neuronal cell types or subtypes.

Pancreatic transcription factor 1a (*Ptf1a*), which encodes a basic helix-loop-helix (bHLH)-type transcription factor, was originally reported as a determiner that drives undifferentiated cells in the foregut endoderm into a pancreatic lineage (Krapp et al., 1998; Kawaguchi et al., 2002). Recently, pivotal roles for *Ptf1a* in nervous system development have been reported, including involvement in

[1]Department of Biochemistry and Cellular Biology, National Institute of Neuroscience, NCNP, Kodaira, Tokyo 187-8502, Japan. [2]Department of Pathology and Tumor Biology, [4]Department of Morphological Brain Science and [7]Department of Surgery, Kyoto University Graduate School of Medicine, Sakyo-ku, Kyoto 606-8501, Japan. [3]Department of Physiology and Cell Biology, Kobe University Graduate School of Medicine, Kobe 650-0017, Japan. [5]Neuronal Circuit Mechanisms Research Group, RIKEN Brain Science Institute, Wako, Saitama 351-0198, Japan. [6]Department of Genetic and Behavioral Neuroscience, Gunma University Graduate School of Medicine, Maebashi 371-8511, Japan.

*Author for correspondence (e-mail: hoshino@ncnp.go.jp)

Accepted 16 April 2009

the development of GABAergic neurons in the cerebellum and dorsal spinal cord (Glasgow et al., 2005; Hoshino et al., 2005), amacrine and horizontal cells in retina (Fujitani et al., 2006; Nakhai et al., 2007) and climbing fiber neurons of the inferior olivary nucleus in the caudal hindbrain (Yamada et al., 2007).

Atonal homolog 1 (*Atoh1*, also called *Math1*), originally cloned as a mammalian homolog of *Drosophila atonal*, also encodes a bHLH-type transcription factor. *Atoh1* has been shown to participate in the development of excitatory neurons in the cerebellum, mossy fiber neurons in the caudal hindbrain, interneurons in the spinal cord, inner ear hair cells and intestinal secretory cells (Bermingham et al., 1999; Bermingham et al., 2001; Yang et al., 2001; Machold and Fishell, 2005; Wang et al., 2005).

In primordia of the cerebellum (r1) and caudal hindbrain (~r6-8), *Atoh1* and *Ptf1a* have been reported to be expressed in discrete neuroepithelial regions in the dorsal half of the neural tube, from which cerebellar and pre-cerebellar (mossy and climbing fiber) neurons are generated. The expression of both genes in ~r2-5 of the hindbrain (Akazawa et al., 1995; Obata et al., 2001), where CN neurons reportedly emerge (Farago et al., 2006), leads us to surmise that CN neurons may be derived from Atoh1- and Ptf1a-expressing regions of the hindbrain.

In a short-term lineage-tracing analysis using *Atoh1-lacZ* knock-in mice, Wang et al. (Wang et al., 2005) observed that cells in the VCN are derived from Atoh1-expressing neuroepithelium, although a small population of *Atoh1*-lineage cells were found to migrate into the DCN (Wang et al., 2005). Our Cre-loxP-based lineage-tracing studies showed that cells derived from Ptf1a-expressing cells were predominantly found in the DCN, although a small number were also observed in the VCN (Yamada et al., 2007). Despite the intermingled localization of *Atoh1*- and *Ptf1a*-lineage cells in both the DCN and VCN, the cell types in each lineage have not been previously investigated.

In this study, through the creation of fate maps of cells in the *Ptf1a* and *Atoh1* lineages, we identified neuroepithelial domains that give rise to inhibitory and excitatory neurons in the CN. We also analyzed phenotypes of the CN in the *Ptf1a* and *Atoh1* mutants. These findings provide clues towards understanding the development of the CN and insights into the molecular machinery that specifies neuron subtypes in the nervous system.

MATERIALS AND METHODS

Animals

All animal experiments in this study have been approved by the Animal Care and Use Committee of the National Institute of Neuroscience, Japan (Project #2008005). The *Ptf1a^{cre}, Rosa26R (R26R)* and *Gad67-GFP (Δneo)* mouse lines were described previously (Soriano, 1999; Kawaguchi et al., 2002; Tamamaki et al., 2003; Hoshino et al., 2005).

Tg-Atoh1-Cre mice were generated using pronuclear injection. *Cre* recombinase cDNA with a methallothionein I polyadenylation signal in pBS185 (Stratagene) was excised by *Xho*I and *Hin*dIII and subcloned into pBluescript (Stratagene) to generate pBS-Cre-polyA. The human β-globin minimal promoter sequence (5′-GGGCTGGGCATAAAAGTCAGGG-CAGACCCATCTATTGCTTACATTTGCTTCTG-3′) whose 5′ and 3′ terminals were tagged with *Kpn*I-*Bgl*II and *Xho*I sites, respectively, was inserted into the cognate sites of pBS-Cre-polyA, generating pBS-pro-Cre-polyA. A 1.6 kb *Atoh1* enhancer in the 3′ UTR of *Atoh1*, similar to that previously described (Helms et al., 2000; Machold and Fishell, 2005) was obtained by PCR from C57BL/6 mouse genomic DNA. Primers used were 5′-TCCAAGGTCCGGCAATGAAGTTTGCATAACAA-3′ and 5′-CCT-CCCCTAGGCTTTGCTTGACTCTGGCTTAA-3′, whose 5′ ends were tagged with *Kpn*I and *Bgl*II restriction sites, respectively. The obtained *Atoh1* enhancer was inserted into *Kpn*I and *Bgl*II sites of pBS-pro-Cre-polyA, producing pAtoh1-Cre, which was used to generate the *Atoh1-Cre* transgenic mouse line. Following CsCl purification of pAtoh1-Cre, a 4.2 kb *Kpn*I-*Hin*dIII fragment was isolated by gel electrophoresis. The fragment was diluted to 3.5 ng/μl and injected into pronuclei of fertilized mouse eggs as reported (Inoue et al., 2008). Nine transgenic founders were established and crossed with *Rosa26R*. Among five lines examined, three revealed strong and precise recapitulation of *Atoh1* expression profiles by X-gal staining in the central nervous system. Two lines were selected for further analysis.

Atoh1^{CreERn} mice were generated as follows. The *Atoh1* locus was targeted with a vector replacing its ORF with the *CreERT2* (Weber et al., 2001) and *neo-resistance* genes (see Fig. S4B in the supplementary material). *CreERT2* encodes a Cre recombinase fused to a mutated estrogen ligand-binding domain (*ERT2*) that requires the presence of tamoxifen for the activity of the fusion protein. In this study, this line was used as a *Atoh1* null allele.

Antibodies and immunohistochemistry

Primary antibodies used in this study were anti-BrdU (1:75; mouse monoclonal; BD, Franklin Lakes, NJ, USA), HuC/D (1:500; mouse monoclonal; Invitrogen, Carlsbad, CA, USA), GFAP (1:1; rabbit; Dakocytomation, Glostrup, Denmark), β-galactosidase (1:800; goat; Biogenesis, Poole, UK), β-galactosidase (1:1600; rabbit; Cappel, Aurora, OH, USA), GABA (1:500; rabbit; Sigma, St Louis, MO, USA), CaMKIIα (1:500; mouse monoclonal; Chemicon, Temecula, CA, USA), glycine (1:1000; rabbit; Chemicon), GFP (1:10; rat; a kind gift from Dr A. Imura, Kyoto University, Kyoto, Japan), Pax6 (1:300; rabbit; Covance, Princeton, USA), Tbr2 (1:5000; rabbit; Chemicon), NR2A (1:500; rabbit; Upstate Biotechnology, USA), NR2B (1:500; rabbit; Upstate), calbindin (1:250; rabbit; Chemicon), calretinin (1:500; rabbit; Chemicon), parvalbumin (1:2500; mouse monoclonal; Sigma), Fluoro-Gold (1:2000; rabbit; Chemicon), Ki67 (1:50; rat; Dako), cleaved caspase 3 (1:100; rabbit; Cell Signaling Technology, Beverly, MA, USA), Mafb (1:500; goat, Santa Cruz, California, USA), Ptf1a (1:1000; rabbit) (Yamada et al., 2007). Immunohistochemistry was performed as described previously (Matsuo et al., 2002; Matsuo et al., 2003; Yoshizawa et al., 2005).

In situ hybridization, X-gal- and activated caspase 3-staining, retrograde labeling and BrdU incorporation

In situ hybridization was performed as described (Hoshino et al., 1999; Yoshizawa et al., 2002; Yoshizawa et al., 2003). The probes used were *Atoh1* (Akazawa et al., 1995) and *VGluT2* (*Slc17a6* – Mouse Genome Informatics) (Nakamura et al., 2008). Detection of β-galactosidase (β-gal) using X-gal, a proteolytically activated form of caspase 3 and retrograde labeling were performed as described (Yamada et al., 2007), and the BrdU incorporation experiment was performed as described (Kawauchi et al., 2003; Kawauchi et al., 2006).

Measurement of widths of the Atoh1 and Ptf1a domains

Atoh1 and Ptf1a domains were visualized by in situ hybridization and immunostaining, respectively. There is a morphologically identifiable notch in the hindbrain neuroepithelium, which is indicated by an arrow in Fig. 1F. This notch is distinct from the sulcus limitans. First, the length between this notch and the dorsalmost tip of the neural neuroepithelium (arrowhead in Fig. 1F) was measured as ‘the dorsal neuroepithelial length’. The ratios of the Atoh1 domain widths to the dorsal neuroepithelial length were 0.370±0.037 and 0.356±0.022 in *Ptf1a$^{cre/+}$* and *Ptf1a$^{cre/cre}$*, respectively (mean±s.d., $P>0.05$, Student’s *t*-test, $n=5$). The ratios of the Ptf1a domain widths to the dorsal neuroepithelial length were 0.291±0.013 and 0.282±0.015 in *Atoh1$^{CreERn/+}$* and *Atoh1$^{CreERn/CreERn}$*, respectively (mean±s.d., $P>0.05$, Student’s *t*-test, $n=4$). These data suggest that the width of the Ptf1a or Atoh1 domain was not affected in the *Ptf1a* or *Atoh1* mutant embryos, either.

RESULTS

Ptf1a is expressed in a discrete neuroepithelial region of the caudal hindbrain

Previous studies suggested that CN neurons are derived from the neuroepithelium in the embryonic ~r2-5 hindbrain region (Farago et al., 2006; Nichols and Bruce, 2006) and that they arise around

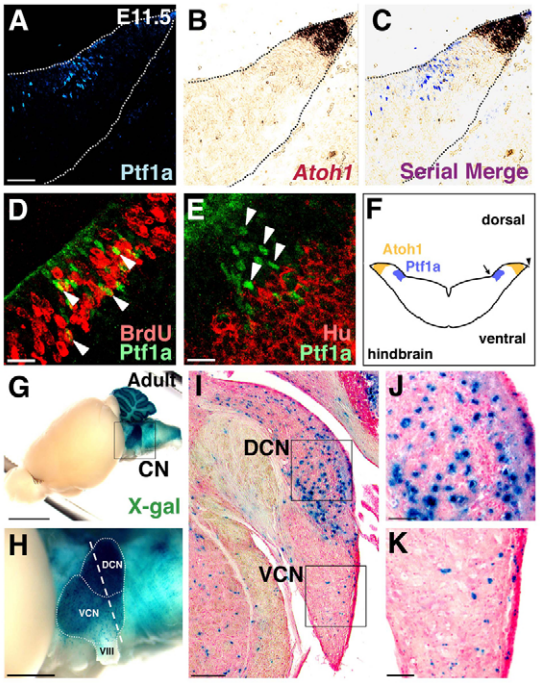

Fig. 1. Expression of Ptf1a and *Atoh1* in the embryonic caudal hindbrain and cells in the *Ptf1a* lineage in adults. (**A-C**) Serial transverse frozen sections of r3 hindbrain at E11.5. Localization of Ptf1a protein (immunohistochemistry) and *Atoh1* transcripts (in situ hybridization) are shown. (**D**) Double immunostaining with Ptf1a (green) and BrdU (red) within the Ptf1a domain at E11.5. Pregnant mice were given BrdU injections 1 hour before embryo harvest and fixation. (**E**) Double immunostaining with Ptf1a and HuC/D at E11.5. (**F**) Schematic diagram of Atoh1 and Ptf1a expression in the middle hindbrain at E11.5. (**G**) Lateral view of a whole-mount X-gal stained brain. The left half of the cerebellum was removed to reveal the CN. (**H**) High magnification of the boxed region in G. (**I**) Transverse section of an X-gal stained brain at the dashed line in H. (**J**,**K**) High magnification of boxed regions in I, DCN and VCN, respectively. Scale bars: A-C, 40 μm; D,E, 20 μm; G, 5 mm; H, 2 mm; I, 200 μm; J,K, 70 μm. CN, cochlear nucleus; DCN, dorsal cochlear nucleus; VCN, ventral cochlear nucleus; VIII, cochlear nerve.

embryonic days (E) 10-14 (Pierce, 1967; Martin and Rickets, 1981; Ivanova and Yuasa, 1998). We investigated the expression of Ptf1a protein in the middle hindbrain (at the r3 level) at E11.5, and compared it with the localization of the *Atoh1* transcript (Fig. 1A,B). As described previously, *Atoh1* was expressed in the dorsal part of the hindbrain (Fig. 1B) (Akazawa et al., 1995; Ben-Arie et al., 1996; Landsberg et al., 2005). Immunostaining of serial sections with an anti-Ptf1a antibody revealed that Ptf1a was expressed in a region located ventral to the *Atoh1*-expressing region (Fig. 1C,F).

BrdU incorporation studies revealed that these Ptf1a-expressing cells contained a mitotic population (arrowheads in Fig. 1D), and correspondingly, immunostaining showed that most were negative for HuC/D, a postmitotic neuronal marker (arrowheads in Fig. 1E), although a few positive cells were observed. These HuC/D-positive cells are likely to have just exited the cell cycle, because they were exclusively found near the ventricular zone and never at the pial side. These findings suggest that the majority of Ptf1a-expressing cells are neuroepithelial cells in the ventricular zone. Ptf1a expression in this region was strongly observed from E11.5 to 13.5 and weakly at E10.5 and 14.5, but was absent after E15.5 (data not shown). A similar pattern of expression was observed in other middle hindbrain regions (r2, 4, 5). In this study, we refer to these Ptf1a- and *Atoh1*-expressing regions as the Ptf1a and Atoh1 neuroepithelial domains.

CN neurons derived from Ptf1a neuroepithelial domain

The *Ptf1a*^{cre} allele was generated by replacement of the *Ptf1a* protein-coding region with that of a Cre recombinase targeted to the nucleus (Kawaguchi et al., 2002). By crossing *Ptf1a*$^{cre/+}$ with *Gt(ROSA)26Sor*^{tm1sor} (*R26R*) mice, which carry a modified *lacZ* gene driven by a cell-type-independent *ROSA26* promoter (Soriano, 1999), we can label *Ptf1a*-expressing cells and their progeny by β-galactosidase (β-gal) detection.

Utilizing this recombination-based lineage-tracing technique, we previously showed that many cells in the DCN as well as a small number of cells in the VCN are derived from Ptf1a-expressing cells (Yamada et al., 2007). Although there are a variety of cells with distinct characteristics in both DCN and VCN, it has not been determined which cell types arise from the Ptf1a domain.

In whole-mount X-gal stained brains of *Ptf1a*$^{cre/+}$*; R26R* adult mice, β-gal signals were strongly and slightly observed in the DCN and VCN, respectively (Fig. 1G,H). We examined serial transverse sections of the CN, which were counterstained with Nuclear Fast Red (Fig. 1I-K). In the DCN, β-gal signals were detected in many cells that were relatively large, whereas relatively small cells were β-gal-negative (Fig. 1J). In the VCN, a small number of cells were labeled with β-gal (Fig. 1K).

Next, we immunostained adult brains of *Ptf1a*$^{cre/+}$*; R26R* mice with β-gal and specific markers (Fig. 2). In both the DCN and VCN, nearly all β-gal-positive cells were found to express HuC/D, a neuronal marker (Fig. 2A, data not shown), but negative for GFAP, a marker for astrocytes (Fig. 2B, data not shown). These findings suggest that most *Ptf1a*-lineage DCN and VCN cells are neurons.

The DCN exhibits a layered structure that contains the ML, the fusiform cell layer (FCL) and the deep layer (DL) (Fig. 4B) (Oertel and Young, 2004). Although there are many types of neurons in the DCN, distinct types of neurons are localized in (a) specific layer(s) (summarized in Fig. 4A). In the DCN, some β-gal-positive cells were immunoreactive to GABA. Their position and morphology suggest that some of these cells in the DL (Fig. 2C, arrowheads) and FCL are Golgi cells (Mugnaini, 1985; Kolston et al., 1992). In addition, a portion of β-gal-positive DCN cells were found to be immunopositive to glycine (Fig. 2D, arrowheads), suggesting that they are tuberculo-ventral cells (Willott et al., 1997; Alibardi, 2006). In the FCL of the DCN, many round β-gal-positive cells express CaMKIIα (Fig. 2E, arrowheads), indicating that cartwheel cells are also in the *Ptf1a*-lineage (Ochiishi et al., 1998; Takaoka et al., 2005). In the ML, some relatively small or mid-sized cells were double stained with β-gal and parvalbumin (Fig. 2F, arrowheads), suggesting that ML-stellate cells are also in the *Ptf1a* lineage (Caicedo et al., 1996), whereas mid-sized, round-shaped cells in the ML and FCL, which are presumably cartwheel cells, also weakly expressed parvalbumin (Fig. 2F).

Glutamate decarboxylase 67 (Gad67; also called Gad1) is expressed in GABA-producing inhibitory neurons (Ribak et al., 1981) and is used as a marker for inhibitory neurons. In the DCN, it has been reported that not only GABAergic (Golgi and ML-stellate) cells but also glycinergic (cartwheel) cells (Golding and Oertel, 1997) express Gad67 (Mugnaini, 1985). Previously, Tamamaki et al. (Tamamaki et al., 2003) generated a *Gad67-GFP* knock-in mouse in which Gad67-expressing cells were labeled by GFP (Tamamaki

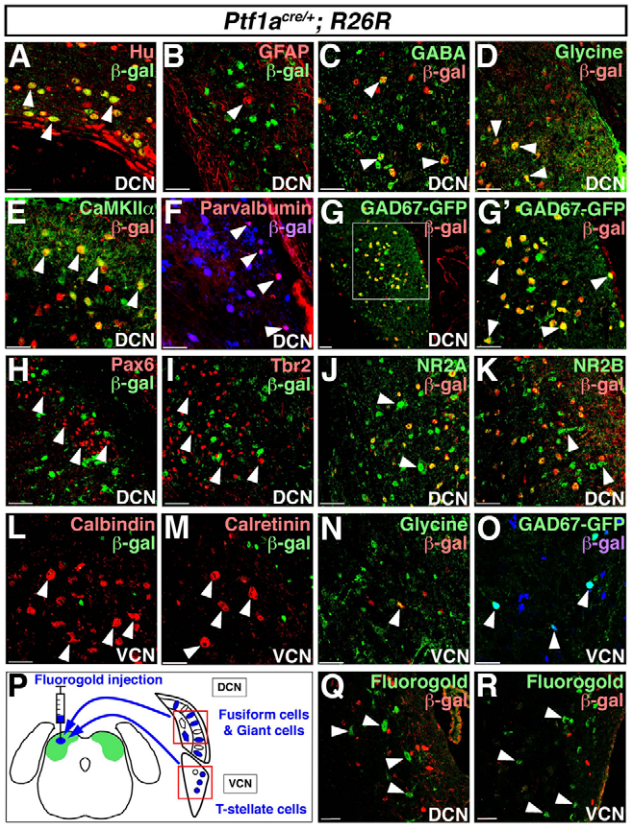

Fig. 2. Cells of the CN in the *Ptf1a* lineage. (**A-O**) Double immunolabeling with indicated antibodies in the adult DCN (A-K) and VCN (L-O) of *Ptf1a*$^{cre/+}$*; R26R* mice. Arrowheads indicate neurons (A), astrocytes (B), and Golgi (C), tuberculo-ventral (D), cartwheel (E), ML-stellate (F), Gad67-GFP-positive (G,O), granule (H), unipolar brush (I), presumable giant (J), presumable fusiform (K), octopus (L), globular-bushy (M) and D-stellate (N) cells. (G′) A high magnification view of the boxed region in G. (**P**) Schematic drawing of Fluoro-Gold retrograde labeling. (**Q**,**R**) Double immunostaining with Fluoro-Gold (green) and β-gal (red) in DCN (Q) and VCN (R). Arrowheads in Q and R indicate fusiform/giant cells and T-stellate cells, respectively. Scale bars: 40 μm.

et al., 2003). We performed co-immunostaining with GFP and markers such as CaMKIIα, GABA and parvalbumin, and confirmed that GFP was expressed in inhibitory neurons including cartwheel, Golgi and ML-stellate cells in the DCN of *Gad67-GFP* mice (see Fig. S1 in the supplementary material). To investigate the cell types in the *Ptf1a* lineage, we analyzed the expression of β-gal in the DCN of *Ptf1a*$^{cre/+}$*; R26R; Gad67-GFP* mice (Fig. 2G,G′). We found that most of the GFP-positive cells were immunoreactive to β-gal in the DCN, revealing that inhibitory neurons, including cartwheel, Golgi and ML-stellate cells, are in the *Ptf1a* lineage.

However, some types of neurons were not labeled with β-gal. Pax6 and Tbr2 (Eomes – Mouse Genome Informatics), markers for granule cells (Weedman et al., 1996; Yamasaki et al., 2001) and unipolar brush cells (Floris et al., 1994; Dino and Mugnaini, 2008), respectively, were not co-stained with β-gal in the DCN (Fig. 2H,I). Although NR2A (Grin2a – Mouse Genome Informatics) is expressed in more than one DCN cell type, giant cells can be easily distinguished by their immunoreactivity to NR2A, localization in the DL, and characteristic large, round morphology (Joelson and Schwartz, 1998). Similarly, fusiform cells can also be discriminated by their expression of NR2B (Grin2b – Mouse Genome Informatics), localization in the FCL and characteristic spindle-like morphology (Petralia et al., 1996). Our immunostaining with NR2A or NR2B in *Ptf1a*$^{cre/+}$*; R26R* mice revealed that giant and fusiform cells do not express β-gal (Fig. 2J,K).

It is known that only two types of neurons in the DCN, giant and fusiform cells, extend their axons to the inferior colliculus (Fig. 2P). We therefore retrogradely labeled giant and fusiform cells by injecting dye into the inferior colliculus (Ryugo and Willard, 1985; Ivanova and Yuasa, 1998; Takaoka et al., 2005). Fluoro-Gold was injected into the inferior colliculus of adult *Ptf1a*$^{cre/+}$*; R26R* mice, which were sacrificed 3 days after injection, followed by immunostaining with anti-Fluoro-Gold and β-gal antibodies. Consistent with the data in Fig. 2J,K, Fluoro-Gold-labeled cells in the DCN did not express β-gal (Fig. 2Q), confirming that giant and fusiform cells in the DCN are not in the *Ptf1a* lineage.

In the VCN, a small number of cells were labeled with β-gal. Double immunolabeling revealed that no β-gal-positive cells expressed calbindin (Frisina et al., 1995) or calretinin (Por et al., 2005), indicating that octopus and globular-bushy cells are not of the *Ptf1a* lineage (Fig. 2L,M). By contrast, some β-gal-positive cells were labeled with glycine (Fig. 2N), suggesting that glycinergic D-stellate cells are in the *Ptf1a* lineage (Wenthold, 1987).

In the VCN of the *Ptf1a*$^{cre/+}$*; R26R; Gad67-GFP* mice, nearly all GFP-positive cells were positive for β-gal, indicating that Gad67-expressing cells in the VCN are in the *Ptf1a* lineage (Fig. 2O). As it has been reported that Gad67 is expressed not only in GABAergic neurons but also in other types of inhibitory neurons (e.g. glycinergic neurons) (Mugnaini, 1985), we believed that Gad67-GFP-positive cells in the VCN might include D-stellate cells. However, Gad67-positive cells may also contain unclassified inhibitory neurons, because the identification and classification of neuronal types are still not complete in the VCN (Hackney et al., 1990).

It is known that T-stellate cells extend their axons to the inferior colliculus (Fig. 2P) (Fujino and Oertel, 2001; Saul et al., 2008). In the retrograde labeling study described in Fig. 2P, Fluoro-Gold-labeled cells in the VCN were not β-gal-positive (Fig. 2R), indicating that T-stellate cells in the VCN are not in the *Ptf1a* lineage.

CN neurons derived from Atoh1 neuroepithelial domain

To genetically label cells that are derived from the Atoh1 neuroepithelial domain, we generated mice (*Tg-Atoh1-Cre*) carrying a transgene that was designed to express Cre recombinase under control of the *Atoh1* enhancer (see Fig. S4A in the supplementary material) (Helms et al., 2000; Machold and Fishell, 2005). In *Tg-Atoh1-Cre; R26R* mice, many β-gal-positive cells were observed in both the anterior and posterior subregions of VCN with relatively fewer β-gal-positive cells in the DCN (Fig. 3A,B), mimicking the distribution pattern previously reported for cells in the *Atoh1* lineage (Wang et al., 2005). In the cerebellum, granule cells and large deep cerebellar nuclei neurons were labeled as previously described (Machold and Fishell, 2005; Wang et al., 2005).

We immunostained adult brains of *Tg-Atoh1-Cre; R26R* mice with β-gal and specific markers to discriminate each cell type (Fig. 3C-K). In the DCN, granule (Fig. 3F, arrowheads) and unipolar brush cells (Fig. 3G, arrowheads) were positive for β-gal, whereas cartwheel (Fig. 3C-E, arrows), Golgi (Fig. 3D, arrowheads) and

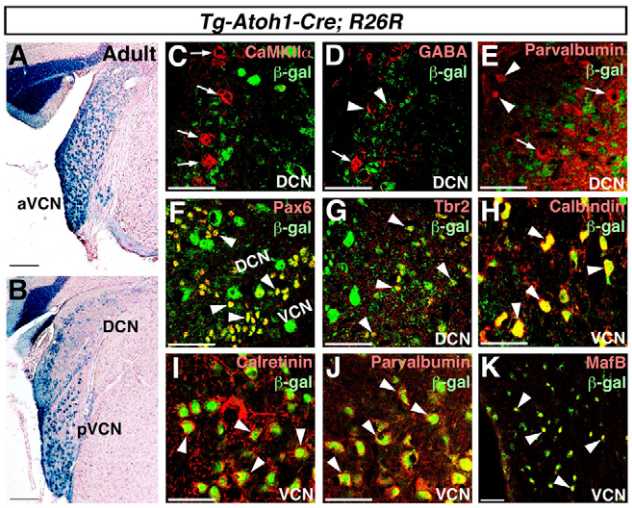

Fig. 3. Cells of the CN in the *Atoh1* lineage. (**A**,**B**) X-gal stained sections of adult *Tg-Atoh1-Cre; R26R* mice at rostral (A) and caudal (B) CN regions. (**C-K**) Double immunolabeling visualized with indicated antibodies in adult DCN (C-G) and VCN (F,H-K) of *Tg-Atoh1-Cre; R26R* mice. Arrowheads indicate Golgi (D), ML-stellate (E), granule (F), unipolar brush (G), octopus (H), globular bushy (I), spherical bushy (J) and Mafb-positive (K) cells. Arrows indicate cartwheel cells (C-E). Scale bars: A,B, 200 μm; C-K, 50 μm.

ML-stellate (Fig. 3E, arrowheads) cells were not. Judging from the position, morphology and immunoreactivity to NR2A and NR2B, respectively, fusiform and giant cells appeared to be positive for β-gal (data not shown). In the VCN, octopus (Fig. 3H, arrowheads), globular bushy (Fig. 3I, arrowheads) and spherical bushy (Fig. 3J, arrowheads) cells expressed β-gal. It is known that Mafb is expressed in many cells in the VCN but not in the DCN (Cordes and Barsh, 1994; Eichmann et al., 1997; Farago et al., 2006). Double immunostaining revealed that most Mafb-positive cells in the VCN were derived from the Atoh1 neuroepithelial domain (Fig. 3K, arrowheads).

The relationship between cell types and their origins is highlighted in Fig. 4. These findings suggest that in the CN, inhibitory (GABAergic or glycinergic) neurons are derived from the Ptf1a neuroepithelial domain, whereas excitatory glutamatergic neurons arise from the Atoh1 domain.

Dorsal origin of Gad67-GFP-positive cells corresponds to Ptf1a neuroepithelial domain of the middle hindbrain

In order to investigate the dynamic movement of inhibitory neurons in the middle hindbrain, we observed Gad67-GFP-positive cells in the *Ptf1a*$^{cre/+}$*; R26R; Gad67-GFP* mice during embryogenesis. At E11.5, GFP-positive cells emerged from two ventricular regions, located dorsally and ventrally (Fig. 5A,A′). The dorsal edge of the dorsally located GFP-positive cells faced the Ptf1a neuroepithelial domain, which was marked with the β-gal-signals (see Fig. S2 in the supplementary material). At this stage, only a few cells outside the ventricular zone were labeled with β-gal, probably because of the time delay (~1 day) between Cre and β-gal expression in this system and because of the relatively faint expression of Ptf1a at earlier stages (e.g. E10.5, data not shown).

At E12.5, whereas some dorsally produced GFP-positive cells migrate ventrally, some of the ventrally generated ones migrate dorsally. These GFP-positive cells never entered the ventricular zone. The majority of dorsally produced GFP-positive cells expressed β-gal (Fig. 5C,C′). These findings suggest that there are two distinct origins of Gad67-GFP positive cells in the middle hindbrain and further indicate that the dorsally located origin corresponds to the Ptf1a neuroepithelial domain.

At E14.5, the GFP-positive cells derived from the two origins become mingled. Some GFP-positive cells, most of which expressed β-gal, were also found at the dorsalmost region of the neural tube, the presumptive CN primordium (Fig. 5E,E′). At E18.5, although many cells double positive for GFP and β-gal were observed in the DCN primordium, a small number of such cells was found in the VCN (Fig. 5G), as observed at the adult stage (Fig. 1I).

Ptf1a is required for CN formation

As the *Ptf1a* null mice (*Ptf1a*$^{cre/cre}$) die just after birth (Kawaguchi et al., 2002), we examined heterozygous and homozygous embryos at E18.5. In Hematoxylin and Eosin (HE)-stained sections, the dorsal region of the CN could not be distinguished in homozygous embryos (Fig. 6A,B). However, many cells positive for Mafb, a marker for VCN neurons, were observed in the mutant CN (Fig. 6C,D). These observations suggest that the DCN is severely disorganized in the *Ptf1a* mutant animals, whereas the VCN is relatively intact.

At E14.5, we observed expansion of a β-gal-positive region facing the ventricular surface in *Ptf1a* homozygous (*Ptf1a*$^{cre/cre}$*; R26R*) embryos (Fig. 6E,F). BrdU incorporation studies showed that

A

	Subtypes	Location	*Ptf1a* lineage	*Atoh1* lineage
Dorsal Cochlear Nucleus				
Golgi cells	GABAergic	FCL and DL	O	X
ML-stellate cells		ML	O	X
Cartwheel cells	glycinergic	ML and FCL	O	X
Tuberculo-ventral cells		DL	O	not tested
Granule cells	glutamatergic	FCL	X	O
Unipolar-brush cells		FCL and DL	X	O
Giant cells		DL	X	O
Fusiform cells		FCL	X	O
Ventral Cochlear Nucleus				
Octopus cells	glutamatergic	mainly pVCN	X	O
Globular-bushy cells		broadly VCN	X	O
Spherical-bushy cells		mainly aVCN	X	O
T-stellate cells		broadly VCN	X	not tested
D-stellate cells	glycinergic	broadly VCN	O	not tested

*DCN…dorsal cochlear nucleus; VCN…ventral cochlear nucleus; aVCN…anterior VCN; pVCN…posterior VCN; FCL…fusiform cell layer; ML…molecular layer; DL …deep layer

B

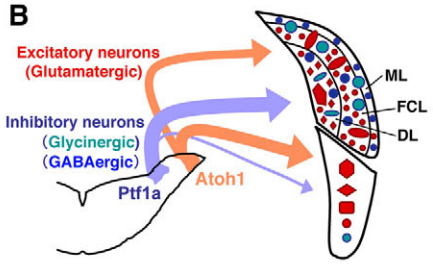

Fig. 4. CN neurons. (**A**) Cell types of CN neurons and their lineages. Neurotransmitter subtypes, cell locations and lineages are indicated. (**B**) Schematic model for lineages of excitatory and inhibitory neurons of the CN.

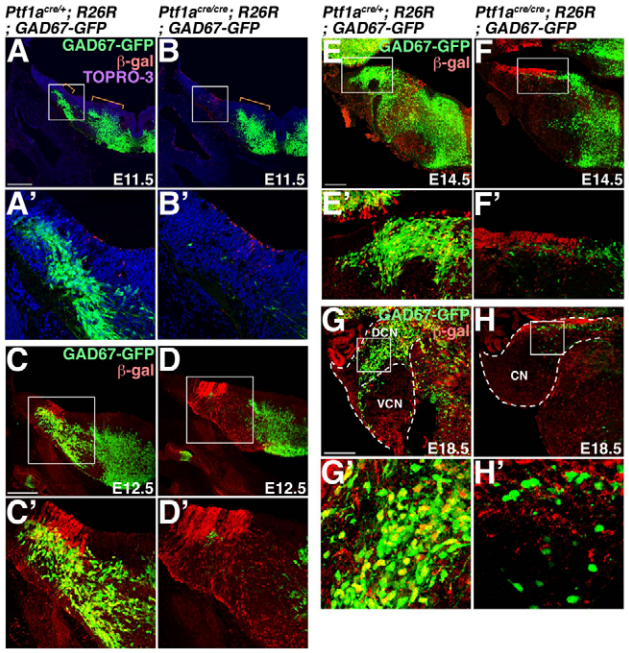

Fig. 5. Dynamics of Gad67-GFP-positive inhibitory neurons and *Ptf1a*-lineage cells during embryogenesis. (**A-H**) Transverse sections of middle hindbrains of indicated genotypes were immunostained with GFP and β-gal. Developmental stages are indicated. In A and B, cell nuclei were visualized by TOPRO3, and brackets indicate dorsally and ventrally located origins of GFP-positive cells. (**A′-H′**) High magnification views of boxed regions in A-H, respectively. Scale bars: 200 μm.

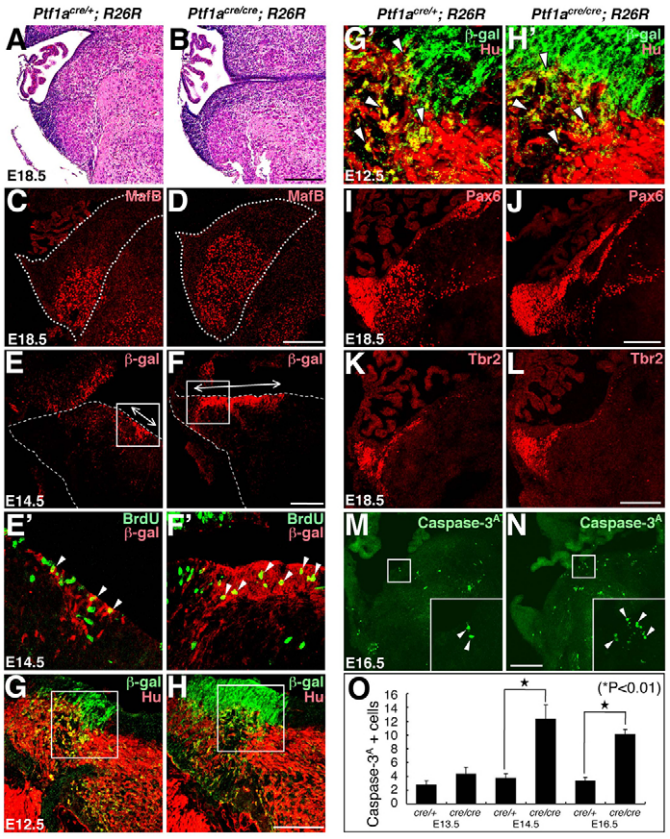

Fig. 6. Phenotypes of the CN in *Ptf1a* mutant embryos. (**A**,**B**) HE-stained transverse sections the CN at E18.5. (**C**,**D**) Hindbrain sections immunostained with Mafb. A white dotted line indicates the outline of the CN primordium. (**E-F′**) Double immunostaining with β-gal and BrdU of E14.5 embryos. Pregnant mice were given BrdU injections 1 hour before embryo harvest and fixation. White dotted lines indicate the outline of the hindbrain. An arrow with two arrowheads in E and F indicates the Ptf1a neuroepithelial domain. (E′,F′) High magnification views of E and F; arrowheads indicate double-labeled cells. (**G**,**H**) Double immunostaining with β-gal and HuC/D to E12.5 hindbrains. (**G′**,**H′**) High magnification views of G and H, arrowheads indicate double-labeled cells. (**I-L**) Immunostaining with Pax6 (I,J) and Tbr2 (K,L) to the E18.5 CN. (**M**,**N**) The CN primordia at E16.5 immunostained with activated caspase 3. Arrowheads in insets indicate apoptotic cells. (**O**) Quantification of the numbers of cleaved caspase 3-positive cells in the CN primordia at E13.5, 14.5 and 16.5. The numbers are 2.75±0.65 and 4.33±0.95 at E13.5, 3.75±1.83 and 12.33±2.02 at E14.5 and 3.35±0.50 and 10.09±0.74 at E16.5 per section in heterozygotes and homozygotes, respectively (mean±s.e.m.), Student's *t*-test, **P*<0.01. *n*=8, 6, 8, 3, 34, 32, respectively. Scale bars: A-F, 200 μm; G,H, 100 μm; I-N, 200 μm.

β-gal-positive cells in this region contain a mitotic population (Fig. 6E′,F′), as further confirmed by immunoreactivity to Ki67, a marker for mitotic cells (data not shown). These results indicate that the ventricular zone expansion occurred with loss of Ptf1a expression. However, β-gal-expressing cells outside the ventricular zone were immunoreactive to HuC/D, a neuronal marker, even in *Ptf1a* homozygous (*Ptf1a*$^{cre/cre}$*; R26R*) embryos (Fig. 6G-H′). In addition, the BrdU incorporation rate was not affected in the *Ptf1a* mutant embryos at E12.5 (see Fig. S3 in the supplementary material). Together, these findings suggest that Ptf1a may be potentially involved in neuronal differentiation rather than in the cell cycle of the neuroepithelial cells.

Next, we examined the distribution of Gad67-GFP-positive cells during various embryonic stages in the *Ptf1a* mutants. In mutants at E11.5, few GFP-positive cells were found in the dorsal region of the neural tube, whereas the number and distribution of GFP-positive cells in the ventral side were not affected (Fig. 5B,B′). At E12.5, although some β-gal-positive cells were found to migrate out of the Ptf1a neuroepithelial domain, most of them did not express GFP (Fig. 5D,D′). Immunostaining with HuC/D suggested that these β-gal-positive/GFP-negative cells possessed neuronal characteristics (Fig. 6H,H′, data not shown). These findings suggest that Ptf1a is required for development of Gad67-GFP-positive cells, presumably inhibitory neurons, which are produced from the Ptf1a neuroepithelial domain in the middle hindbrain.

At E14.5, a stream of GFP-positive cells was observed to intrude into the dorsal neural tube beneath the β-gal-expressing neuroepithelial region (Fig. 5F,F′). Because these GFP-positive cells never co-localized with β-gal, they were probably neurons from the ventral region. At E18.5, few GFP-positive cells were observed in the mutant CN, except for the proximal edge (Fig. 5H), indicating that Ptf1a is required for development of inhibitory neurons in the CN. Although a small number of GFP-positive cells were found at the proximal edge of the CN, these cells were not marked with β-gal (Fig. 5H′), suggesting that these were derived from the ventral region.

However, we observed many Pax6- and Tbr2-positive cells in the Ptf1a mutant CN at E18.5 (Fig. 6I-L), suggesting that glutamatergic granule and unipolar brush cells were not affected by loss of Ptf1a expression. In the central region of the CN in *Ptf1a* mutants, few β-gal-positive cells were found at E18.5 (Fig. 5H), although a

considerable number were observed at E14.5 (Fig. 5F, data not shown). To determine if increased apoptosis was occurring, we used an antibody against the proteolytically activated form of caspase 3 (Fernandes-Alnemri et al., 1994; Ura et al., 2001). At E14.5 and 16.5, approximately threefold more apoptotic cells were found in the dorsolateral region of the middle hindbrain (that is, the CN primordium) of the mutants compared with the heterozygotes (Fig. 6M-O).

In addition, we investigated whether the width of the Atoh1 domain is changed in the *Ptf1a* mutant embryos. In situ hybridization with the *Atoh1* probe to the E11.5 embryos revealed that the width of the Atoh1 domain is not affected in the *Ptf1a* mutants (see Materials and methods).

Cochlear nucleus in the *Atoh1* mutants

To investigate the role of *Atoh1* in CN formation, we generated an *Atoh1* mutant allele ($Atoh1^{CreERn}$) in which the open reading frame of the *Atoh1* gene is replaced with a cDNA encoding CreERT2 (see Fig. S4B in the supplementary material) (Weber et al., 2001). No expression of *Atoh1* was detected by RT-PCR analysis in the homozygous neural tube (see Fig. S4C in the supplementary material), confirming that $Atoh1^{CreERn}$ is a null allele. As the *Atoh1* homozygous null mice die within several minutes after birth (Ben-Arie et al., 1997), we examined wild-type and homozygous embryos ($Atoh1^{CreERn/CreERn}$) at E18.5.

In HE-stained sections, the ventral CN was indiscernible in the homozygous embryos (Fig. 7A,B), as previously reported for another *Atoh1* null allele (Wang et al., 2005), with few Mafb-positive cells observed (Fig. 7C,D). Granule cells, which can be recognized by their small round shape and Pax6 expression, and unipolar brush cells (positive for Tbr2) were also extremely reduced in the mutant CN (Fig. 7E-H).

To investigate the distribution of glutamatergic neurons in the CN, we performed in situ hybridization with *VGluT2* (Fig. 7I) (Fremeau et al., 2001; Nakamura et al., 2008). In the *Atoh1* null embryos ($Atoh1^{CreERn/CreERn}$), few *VGluT2*-expressing cells were observed in what remained of the CN, which probably corresponds to the DCN (Fig. 7J). By contrast, GABA-positive inhibitory neurons were maintained in the *Atoh1* mutant CN (Fig. 7K,L).

To study the fate of *Atoh1*-lineage cells in the *Atoh1* mutants, pregnant mice were given an oral administration of 6 mg tamoxifen and their progenies ($Atoh1^{CreERn/+}$; *R26R* or $Atoh1^{CreERn/CreERn}$; *R26R*) were sacrificed at E18.5 for further analyses (see Fig. S5 in the supplementary material). In mice carrying the $Atoh1^{CreERn}$ allele, CreERT2 is designed to be expressed under the control of the *Atoh1* promoter, which theoretically enables the visualization of the *Atoh1*-lineage cells by β-gal expression from the *R26R* allele (Weber et al., 2001). In our experimental conditions, the number of labeled cells was smaller than expected (see Fig. S5A,A′ in the supplementary material), due to unknown reasons. However, double immunostaining with β-gal and other markers revealed that those β-gal-positive cells were exclusively in the *Atoh1* lineage (data not shown). Interestingly, many β-gal-positive cells were observed in the choroid plexus in the mutants, but were rarely detected there in the heterozygotes (see Fig. S5B,B′ in the supplementary material). Double immunostaining revealed that the β-gal-labeled cells were not positive for GABA in the *Atoh1* heterozygotes and homozygotes (see Fig. S5C-D′ in the supplementary material). However, some β-gal-positive cells in the *Atoh1* mutants were expressing parvalbumin (see Fig. S5E-F′ in the supplementary material), a marker for cartwheel and ML-stellate cells, which were not observed in the heterozygotes. These data suggest that the *Atoh1*-mutant cells might acquire partial characteristics of cartwheel and/or ML-stellate cells, although they did not seem to obtain full features, such as GABA-positivity.

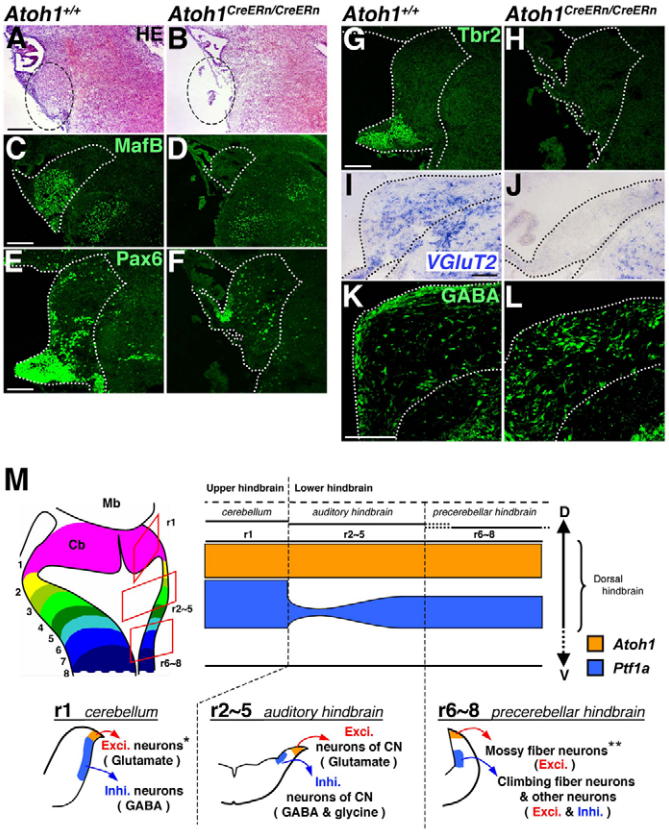

Fig. 7. Phenotypes of the CN in *Atoh1* mutants at E18.5. (**A-L**) Genotypes are indicated. (A,B) HE-stained transverse sections of the CN at E18.5. A black dotted line in A indicates the VCN primordium, which is not observed in B. (C-H,K,L) Hindbrain sections at E18.5 immunostained with indicated antibodies. (I,J) In situ hybridization of E18.5 CN with *VGluT2* probe. White and black dotted lines in C-L highlight outlines of the CN primordia. (**M**) Atoh1 and Ptf1a neuroepithelial domains in the entire hindbrain. (M, left upper panel) Schematic picture of the dorsal rhombomeric structure. Each number represents the rhombomeric number. (M, right upper panel) The Atoh1 and Ptf1a domains throughout the hindbrain (r1~8) are shown. Upper side is dorsal, lower is ventral. (M, lower panels) Schematic pictures corresponding to orange rectangular sections in the left upper panel, which show neuronal subtypes originated from distinct neuroepithelial domains. *(Hoshino et al., 2005; Wang et al., 2005; Machold and Fishell, 2005). **(Wang et al., 2005; Yamada et al., 2007; Landsberg et al., 2006). Scale bars: A-D, 200 μm; E-L, 100 μm. Cb, cerebellum; Exci., excitatory neurons; Inhi., inhibitory neurons; Mb, midbrain.

In addition, we investigated whether the width of the Ptf1a domain is changed in the *Atoh1* mutant embryos. Immunostaining with Ptf1a in the E11.5 embryos revealed that the width of the Ptf1a domain was not affected in the *Atoh1* mutants (see Materials and methods).

These observations suggest that *Atoh1* is involved in development of glutamatergic excitatory neurons of both VCN and DCN, but not inhibitory neurons in the CN, consistent with our lineage-analysis results (Fig. 4A). Because the majority of VCN neurons are glutamatergic, the VCN structure may be much more severely affected than the DCN in the *Atoh1* mutants.

DISCUSSION

In this study, we identified two neuroepithelial domains in the dorsal part of the hindbrain (~r2-5) that express Ptf1a and Atoh1, respectively. Using Cre-loxP-based genetic-fate-mapping studies, we showed that GABAergic and glycinergic inhibitory neurons of both the DCN and the VCN are derived from the Ptf1a domain. Furthermore, we revealed two distinct origins for Gad67-GFP-positive inhibitory neurons in the middle hindbrain (~r2-5), one dorsal and the other ventral. The dorsally located origin corresponds to the Ptf1a neuroepithelial domain. These findings suggest that the Ptf1a neuroepithelial domain generates dorsally produced inhibitory neurons of the middle hindbrain (~r2-5), some of which give rise to inhibitory neurons of the CN.

In the *Ptf1a*-null embryos, Gad67-GFP-labeled inhibitory neurons were hardly produced from the dorsal region, whereas ventrally generated ones were not affected. This confirms that the dorsal origin is precisely coincident with the Ptf1a neuroepithelial domain and suggests that Ptf1a is required for development of these inhibitory neurons.

As to the CN, the dorsal region was severely disorganized in the *Ptf1a* null embryos, whereas the ventral part seemed to be relatively intact. However, even in the ventral part, Gad67-GFP-labeled inhibitory neurons were lost in the mutant embryos. By contrast, the glutamatergic population seemed to be maintained in the mutant CN. As inhibitory neurons were predominantly localized in the DCN, the DCN might be affected more severely than the VCN in the *Ptf1a* mutants. In the CN primordia at E14.5 and 16.5, increased apoptosis was present in the mutants, probably leading to a severe reduction of *Ptf1a*-lineage cells in the CN at later developmental stages. These facts indicate that Ptf1a is involved in differentiation and survival of inhibitory neurons in the CN.

Consequently, Ptf1a participates in the development of inhibitory neurons in the cerebellum (Hoshino et al., 2005), the spinal cord (Glasgow et al., 2005) and the CN. Moreover, we previously showed that ectopically expressed Ptf1a in the dorsal telencephalon neuroepithelium can confer GABAergic characteristics on the progeny neurons. However, the underlying molecular machinery to specify inhibitory fate has not been clarified. By contrast, this gene is also involved in the development of non-inhibitory neurons, such as climbing fiber neurons in the inferior olivary nucleus (Yamada et al., 2007) and some types of amacrine cells in the retina (Fujitani et al., 2006). Altogether, these facts suggest a very complex function of Ptf1a, through which cells can differentiate into inhibitory or other types of neurons, depending on the spatial information in the brain.

Previously, short-term lineage analyses in mice with a β-gal reporter inserted in the *Atoh1* locus reported that the Atoh1 neuroepithelial domain dominantly produced neurons of the VCN plus granule cells in the CN (Wang et al., 2005). However, the specific subtypes of cells in the *Atoh1* lineage were not identified. Our Cre-loxP recombination-based lineage-trace analysis revealed that the Atoh1 neuroepithelial domain generates glutamatergic excitatory neurons in the CN. We think our findings are not contradictory to those reported by Wang et al. (Wang et al., 2005), because they also observed a small population of cells in the *Atoh1* lineage that migrated into the DCN.

Furthermore, we analyzed the phenotypes of *Atoh1* null embryos. As previously reported (Wang et al., 2005), we found that the structure of the mutant VCN was severely disorganized, with loss of Mafb-positive cells, whereas the DCN was relatively intact. However, even in the relatively intact part of the CN (dorsal CN), granule cells, unipolar brush cells and *VGluT2*-expressing glutamatergic neurons were severely reduced in the *Atoh1* mutants. These findings suggest that Atoh1 is involved in CN glutamatergic neuron development.

Inhibitory and excitatory neurons in the CN are derived from distinct regions: the Ptf1a and Atoh1 neuroepithelial domains of the middle hindbrain, respectively (Fig. 4B). It is possible that this correlation may also be applied to cerebellar development. In the part of the cerebellum that corresponds to the dorsal region of rostral hindbrain (r1), inhibitory and excitatory neurons are produced from the Ptf1a- and Atoh1-expressing neuroepithelial regions, respectively, and their development is dependent on the corresponding bHLH proteins.

By contrast, this rule is not applicable to the caudal hindbrain. We previously showed that the Ptf1a neuroepithelial domain in the caudal hindbrain (~r6-8) produces not only inhibitory but also excitatory neurons, such as inferior olivary neurons, the solo source of the climbing fibers (Yamada et al., 2007). In addition, Farago et al. (Farago et al., 2006) named the dorsal regions of the middle (r2-5) and caudal (r6-8) hindbrain as ‘auditory lip’ and ‘pre-cerebellar lip’, respectively, as these two subdomains generate distinct sets of neurons; the former generates CN neurons and the latter pre-cerebellar neurons, such as mossy and climbing fiber neurons. These facts suggest that middle (~r2-5) and caudal (~r6-8) hindbrain subdomains have distinct characteristics. Accordingly, in the middle hindbrain, we did not observe an intervention of neurogenin 1-expressing neuroepithelial domain between the Ptf1a and Atoh1 domains (data not shown), which exists in the caudal hindbrain (Landsberg et al., 2005; Yamada et al., 2007). Overall, throughout the hindbrain regions from r1 to r8, the bHLH type transcription factors, Ptf1a and Atoh1, seem to define neuroepithelial domains along the dorsoventral axis and participate in specifying distinct neuron subtypes according to the rostrocaudal spatial information (Fig. 7M).

The DCN and the VCN have distinct anatomical structures. The DCN exhibits a laminar and cerebellum-like organization that includes a granule cell system (Mugnaini et al., 1980b; Mugnaini et al., 1980a; Oertel and Young, 2004). By contrast, the VCN does not have a laminar structure. Therefore, it has been proposed that developmental machinery for these two nuclei is quite different. On the one hand, in this study, we revealed that neurons with the same electrophysical nature (e.g. inhibitory or excitatory) in both nuclei are derived from the same neuroepithelial domain, which is dorsoventrally defined by a bHLH transcription factor, Ptf1a or Atoh1. On the other hand, Farago et al. (Farago et al., 2006) showed that VCN and DCN neurons are produced from ~r2-4 and r4, 5 of the hindbrain, although some overlap was observed. We observed that the Ptf1a domain is relatively narrower in ~r2-3 than ~r4-5 (data not shown). This may account for the smaller number of inhibitory neurons in the VCN that are derived from the Ptf1a domain. Thus, CN cell types seem to be determined according to rostrocaudal and dorsoventral spatial information of the neuroepithelium.

The CN contains a variety of neurons, each of which has distinct morphological, histochemical and physiological characteristics. Although we have clarified the molecular mechanisms to specify electrophysiological subtypes (inhibitory or excitatory) of CN neurons, the question still remains as to how distinct types of inhibitory neurons in the CN (e.g. cartwheel, Golgi, ML-stellate, etc.) are differentially generated from the Ptf1a neuroepithelial domain or how distinct types of excitatory ones (e.g. fusiform, granule, octopus cells) are differentially produced from the Atoh1 domain. Further studies are required to uncover the molecular

machinery that specifies each cell type in the CN, which may lead to a better understanding of the common mechanisms that govern development of CNS neurons.

We thank T. Obata for technical assistance, H. Kumanogoh for experimental support, A. Watakabe and T. Yamamori for technical information, C. V. E. Wright for *Ptf1a*^{cre} mice, P. Soriano and R. Behringer for *R26R* mice, R. Kageyama for the *Atoh1* probe and R. Yu for helpful discussions, P. Chambon and IGBMC (CNRS/INSERM/ULP) for providing us with the CreERT2 plasmid. This work was supported by grants from the MEXT and the Uehara Memorial Foundation.

Supplementary material

Supplementary material for this article is available at http://dev.biologists.org/cgi/content/full/136/12/2049/DC1

References

Akazawa, C., Ishibashi, M., Shimizu, C., Nakanishi, S. and Kageyama, R. (1995). A mammalian helix-loop-helix factor structurally related to the product of Drosophila proneural gene atonal is a positive transcriptional regulator expressed in the developing nervous system. *J. Biol. Chem.* **270**, 8730-8738.

Alibardi, L. (2006). Review: cytological characteristics of commissural and tuberculo-ventral neurons in the rat dorsal cochlear nucleus. *Hear. Res.* **216-217**, 73-80.

Ben-Arie, N., McCall, A. E., Berkman, S., Eichele, G., Bellen, H. J. and Zoghbi, H. Y. (1996). Evolutionary conservation of sequence and expression of the bHLH protein Atonal suggests a conserved role in neurogenesis. *Hum. Mol. Genet.* **5**, 1207-1216.

Ben-Arie, N., Bellen, H. J., Armstrong, D. L., McCall, A. E., Gordadze, P. R., Guo, Q., Matzuk, M. M. and Zoghbi, H. Y. (1997). Math1 is essential for genesis of cerebellar granule neurons. *Nature* **390**, 169-172.

Bermingham, N. A., Hassan, B. A., Price, S. D., Vollrath, M. A., Ben-Arie, N., Eatock, R. A., Bellen, H. J., Lysakowski, A. and Zoghbi, H. Y. (1999). Math1: an essential gene for the generation of inner ear hair cells. *Science* **284**, 1837-1841.

Bermingham, N. A., Hassan, B. A., Wang, V. Y., Fernandez, M., Banfi, S., Bellen, H. J., Fritzsch, B. and Zoghbi, H. Y. (2001). Proprioceptor pathway development is dependent on Math1. *Neuron* **30**, 411-422.

Caicedo, A., d'Aldin, C., Puel, J. L. and Eybalin, M. (1996). Distribution of calcium-binding protein immunoreactivities in the guinea pig auditory brainstem. *Anat. Embryol. (Berl.)* **194**, 465-487.

Cambronero, F. and Puelles, L. (2000). Rostrocaudal nuclear relationships in the avian medulla oblongata: a fate map with quail chick chimeras. *J. Comp. Neurol.* **427**, 522-545.

Cordes, S. P. and Barsh, G. S. (1994). The mouse segmentation gene kr encodes a novel basic domain-leucine zipper transcription factor. *Cell* **79**, 1025-1034.

Cramer, K. S., Fraser, S. E. and Rubel, E. W. (2000). Embryonic origins of auditory brain-stem nuclei in the chick hindbrain. *Dev. Biol.* **224**, 138-151.

Dino, M. R. and Mugnaini, E. (2008). Distribution and phenotypes of unipolar brush cells in relation to the granule cell system of the rat cochlear nucleus. *Neuroscience* **154**, 29-50.

Eichmann, A., Grapin-Botton, A., Kelly, L., Graf, T., Le Douarin, N. M. and Sieweke, M. (1997). The expression pattern of the mafB/kr gene in birds and mice reveals that the kreisler phenotype does not represent a null mutant. *Mech. Dev.* **65**, 111-122.

Farago, A. F., Awatramani, R. B. and Dymecki, S. M. (2006). Assembly of the brainstem cochlear nuclear complex is revealed by intersectional and subtractive genetic fate maps. *Neuron* **50**, 205-218.

Fernandes-Alnemri, T., Litwack, G. and Alnemri, E. S. (1994). CPP32, a novel human apoptotic protein with homology to Caenorhabditis elegans cell death protein Ced-3 and mammalian interleukin-1 beta-converting enzyme. *J. Biol. Chem.* **269**, 30761-30764.

Floris, A., Dino, M., Jacobowitz, D. M. and Mugnaini, E. (1994). The unipolar brush cells of the rat cerebellar cortex and cochlear nucleus are calretinin-positive: a study by light and electron microscopic immunocytochemistry. *Anat. Embryol. (Berl.)* **189**, 495-520.

Fremeau, R. T., Jr, Troyer, M. D., Pahner, I., Nygaard, G. O., Tran, C. H., Reimer, R. J., Bellocchio, E. E., Fortin, D., Storm-Mathisen, J. and Edwards, R. H. (2001). The expression of vesicular glutamate transporters defines two classes of excitatory synapse. *Neuron* **31**, 247-260.

Frisina, R. D., Zettel, M. L., Kelley, P. E. and Walton, J. P. (1995). Distribution of calbindin D-28k immunoreactivity in the cochlear nucleus of the young adult chinchilla. *Hear. Res.* **85**, 53-68.

Fujino, K. and Oertel, D. (2001). Cholinergic modulation of stellate cells in the mammalian ventral cochlear nucleus. *J. Neurosci.* **21**, 7372-7383.

Fujitani, Y., Fujitani, S., Luo, H., Qiu, F., Burlison, J., Long, Q., Kawaguchi, Y., Edlund, H., MacDonald, R. J., Furukawa, T. et al. (2006). Ptf1a determines horizontal and amacrine cell fates during mouse retinal development. *Development* **133**, 4439-4450.

Glasgow, S. M., Henke, R. M., Macdonald, R. J., Wright, C. V. and Johnson, J. E. (2005). Ptf1a determines GABAergic over glutamatergic neuronal cell fate in the spinal cord dorsal horn. *Development* **132**, 5461-5469.

Golding, N. L. and Oertel, D. (1997). Physiological identification of the targets of cartwheel cells in the dorsal cochlear nucleus. *J. Neurophysiol.* **78**, 248-260.

Hackney, C. M., Osen, K. K. and Kolston, J. (1990). Anatomy of the cochlear nuclear complex of guinea pig. *Anat. Embryol. (Berl.)* **182**, 123-149.

Helms, A. W., Abney, A. L., Ben-Arie, N., Zoghbi, H. Y. and Johnson, J. E. (2000). Autoregulation and multiple enhancers control Math1 expression in the developing nervous system. *Development* **127**, 1185-1196.

Hoshino, M. (2006). Molecular machinery governing GABAergic neuron specification in the cerebellum. *Cerebellum* **5**, 193-198.

Hoshino, M., Suzuki, E., Miyake, T., Sone, M., Komatsu, A., Nabeshima, Y. and Hama, C. (1999). Neural expression of hikaru genki protein during embryonic and larval development of Drosophila melanogaster. *Dev. Genes Evol.* **209**, 1-9.

Hoshino, M., Nakamura, S., Mori, K., Kawauchi, T., Terao, M., Nishimura, Y. V., Fukuda, A., Fuse, T., Matsuo, N., Sone, M. et al. (2005). Ptf1a, a bHLH transcriptional gene, defines GABAergic neuronal fates in cerebellum. *Neuron* **47**, 201-213.

Inoue, T., Inoue, Y. U., Asami, J., Izumi, H., Nakamura, S. and Krumlauf, R. (2008). Analysis of mouse Cdh6 gene regulation by transgenesis of modified bacterial artificial chromosomes. *Dev. Biol.* **315**, 506-520.

Ivanova, A. and Yuasa, S. (1998). Neuronal migration and differentiation in the development of the mouse dorsal cochlear nucleus. *Dev. Neurosci.* **20**, 495-511.

Joelson, D. and Schwartz, I. R. (1998). Development of N-methyl-D-aspartate receptor subunit immunoreactivity in the neonatal gerbil cochlear nucleus. *Microsc. Res. Tech.* **41**, 246-262.

Kawaguchi, Y., Cooper, B., Gannon, M., Ray, M., MacDonald, R. J. and Wright, C. V. (2002). The role of the transcriptional regulator Ptf1a in converting intestinal to pancreatic progenitors. *Nat. Genet.* **32**, 128-134.

Kawauchi, T., Chihama, K., Nabeshima, Y. and Hoshino, M. (2003). The *in vivo* roles of STEF/Tiam1, Rac1 and JNK in cortical neuronal migration. *EMBO J.* **22**, 4190-4201.

Kawauchi, T., Chihama, K., Nabeshima, Y. and Hoshino, M. (2006). Cdk5 phosphorylates and stabilizes p27kip1 contributing to actin organization and cortical neuronal migration. *Nat. Cell Biol.* **8**, 17-26.

Kolston, J., Osen, K. K., Hackney, C. M., Ottersen, O. P. and Storm-Mathisen, J. (1992). An atlas of glycine- and GABA-like immunoreactivity and colocalization in the cochlear nuclear complex of the guinea pig. *Anat. Embryol. (Berl.)* **186**, 443-465.

Krapp, A., Knofler, M., Ledermann, B., Burki, K., Berney, C., Zoerkler, N., Hagenbuchle, O. and Wellauer, P. K. (1998). The bHLH protein PTF1-p48 is essential for the formation of the exocrine and the correct spatial organization of the endocrine pancreas. *Genes Dev.* **12**, 3752-3763.

Landsberg, R. L., Awatramani, R. B., Hunter, N. L., Farago, A. F., DiPietrantonio, H. J., Rodriguez, C. I. and Dymecki, S. M. (2005). Hindbrain rhombic lip is comprised of discrete progenitor cell populations allocated by Pax6. *Neuron* **48**, 933-947.

Machold, R. and Fishell, G. (2005). Math1 is expressed in temporally discrete pools of cerebellar rhombic-lip neural progenitors. *Neuron* **48**, 17-24.

Martin, M. R. and Rickets, C. (1981). Histogenesis of the cochlear nucleus of the mouse. *J. Comp. Neurol.* **197**, 169-184.

Matsuo, N., Hoshino, M., Yoshizawa, M. and Nabeshima, Y. (2002). Characterization of STEF, a guanine nucleotide exchange factor for Rac1, required for neurite growth. *J. Biol. Chem.* **277**, 2860-2868.

Matsuo, N., Terao, M., Nabeshima, Y. and Hoshino, M. (2003). Roles of STEF/Tiam1, guanine nucleotide exchange factors for Rac1, in regulation of growth cone morphology. *Mol. Cell Neurosci.* **24**, 69-81.

Mugnaini, E. (1985). GABA neurons in the superficial layers of the rat dorsal cochlear nucleus: light and electron microscopic immunocytochemistry. *J. Comp. Neurol.* **235**, 61-81.

Mugnaini, E., Warr, W. B. and Osen, K. K. (1980a). Distribution and light microscopic features of granule cells in the cochlear nuclei of cat, rat, and mouse. *J. Comp. Neurol.* **191**, 581-606.

Mugnaini, E., Osen, K. K., Dahl, A. L., Friedrich, V. L., Jr and Korte, G. (1980b). Fine structure of granule cells and related interneurons (termed Golgi cells) in the cochlear nuclear complex of cat, rat and mouse. *J. Neurocytol.* **9**, 537-570.

Nakamura, K., Watakabe, A., Hioki, H., Fujiyama, F., Tanaka, Y., Yamamori, T. and Kaneko, T. (2008). Transiently increased colocalization of vesicular glutamate transporters 1 and 2 at single axon terminals during postnatal development of mouse neocortex: a quantitative analysis with correlation coefficient. *Eur. J. Neurosci.* **28**, 1032-1046.

Nakhai, H., Sel, S., Favor, J., Mendoza-Torres, L., Paulsen, F., Duncker, G. I. and Schmid, R. M. (2007). Ptf1a is essential for the differentiation of GABAergic and glycinergic amacrine cells and horizontal cells in the mouse retina. *Development* **134**, 1151-1160.

Nichols, D. H. and Bruce, L. L. (2006). Migratory routes and fates of cells transcribing the Wnt-1 gene in the murine hindbrain. *Dev. Dyn.* **235**, 285-300.
Obata, J., Yano, M., Mimura, H., Goto, T., Nakayama, R., Mibu, Y., Oka, C. and Kawaichi, M. (2001). p48 subunit of mouse PTF1 binds to RBP-Jkappa/CBF-1, the intracellular mediator of Notch signalling, and is expressed in the neural tube of early stage embryos. *Genes Cells* **6**, 345-360.
Ochiishi, T., Yamauchi, T. and Terashima, T. (1998). Regional differences between the immunohistochemical distribution of Ca^{2+}/calmodulin-dependent protein kinase II alpha and beta isoforms in the brainstem of the rat. *Brain Res.* **790**, 129-140.
Oertel, D. and Young, E. D. (2004). What's a cerebellar circuit doing in the auditory system? *Trends Neurosci.* **27**, 104-110.
Osen, K. K. (1969). Cytoarchitecture of the cochlear nuclei in the cat. *J. Comp. Neurol.* **136**, 453-484.
Petralia, R. S., Wang, Y. X., Zhao, H. M. and Wenthold, R. J. (1996). Ionotropic and metabotropic glutamate receptors show unique postsynaptic, presynaptic, and glial localizations in the dorsal cochlear nucleus. *J. Comp. Neurol.* **372**, 356-383.
Pierce, E. T. (1967). Histogenesis of the dorsal and ventral cochlear nuclei in the mouse. An autoradiographic study. *J. Comp. Neurol.* **131**, 27-54.
Por, A., Pocsai, K., Rusznak, Z. and Szucs, G. (2005). Presence and distribution of three calcium binding proteins in projection neurons of the adult rat cochlear nucleus. *Brain Res.* **1039**, 63-74.
Ribak, C. E., Vaughn, J. E. and Barber, R. P. (1981). Immunocytochemical localization of GABAergic neurones at the electron microscopical level. *Histochem. J.* **13**, 555-582.
Ross, S. E., Greenberg, M. E. and Stiles, C. D. (2003). Basic helix-loop-helix factors in cortical development. *Neuron* **39**, 13-25.
Ryugo, D. K. and Willard, F. H. (1985). The dorsal cochlear nucleus of the mouse: a light microscopic analysis of neurons that project to the inferior colliculus. *J. Comp. Neurol.* **242**, 381-396.
Saul, S. M., Brzezinski, J. A. t., Altschuler, R. A., Shore, S. E., Rudolph, D. D., Kabara, L. L., Halsey, K. E., Hufnagel, R. B., Zhou, J., Dolan, D. F. et al. (2008). Math5 expression and function in the central auditory system. *Mol. Cell Neurosci.* **37**, 153-169.
Soriano, P. (1999). Generalized lacZ expression with the ROSA26 Cre reporter strain. *Nat. Genet.* **21**, 70-71.
Takaoka, Y., Setsu, T., Misaki, K., Yamauchi, T. and Terashima, T. (2005). Expression of reelin in the dorsal cochlear nucleus of the mouse. *Brain Res. Dev. Brain Res.* **159**, 127-134.
Tamamaki, N., Yanagawa, Y., Tomioka, R., Miyazaki, J., Obata, K. and Kaneko, T. (2003). Green fluorescent protein expression and colocalization with calretinin, parvalbumin, and somatostatin in the GAD67-GFP knock-in mouse. *J. Comp. Neurol.* **467**, 60-79.
Tan, K. and Le Douarin, N. M. (1991). Development of the nuclei and cell migration in the medulla oblongata. Application of the quail-chick chimera system. *Anat. Embryol. (Berl.)* **183**, 321-343.
Ura, S., Masuyama, N., Graves, J. D. and Gotoh, Y. (2001). MST1-JNK promotes apoptosis via caspase-dependent and independent pathways. *Genes Cells* **6**, 519-530.
Wang, V. Y., Rose, M. F. and Zoghbi, H. Y. (2005). Math1 expression redefines the rhombic lip derivatives and reveals novel lineages within the brainstem and cerebellum. *Neuron* **48**, 31-43.
Weber, P., Metzger, D. and Chambon, P. (2001). Temporally controlled targeted somatic mutagenesis in the mouse brain. *Eur. J. Neurosci.* **14**, 1777-1783.
Weedman, D. L., Pongstaporn, T. and Ryugo, D. K. (1996). Ultrastructural study of the granule cell domain of the cochlear nucleus in rats: mossy fiber endings and their targets. *J. Comp. Neurol.* **369**, 345-360.
Wenthold, R. J. (1987). Evidence for a glycinergic pathway connecting the two cochlear nuclei: an immunocytochemical and retrograde transport study. *Brain Res.* **415**, 183-187.
Willott, J. F., Milbrandt, J. C., Bross, L. S. and Caspary, D. M. (1997). Glycine immunoreactivity and receptor binding in the cochlear nucleus of C57BL/6J and CBA/CaJ mice: effects of cochlear impairment and aging. *J. Comp. Neurol.* **385**, 405-414.
Wilson, S. W. and Rubenstein, J. L. (2000). Induction and dorsoventral patterning of the telencephalon. *Neuron* **28**, 641-651.
Yamada, M., Terao, M., Terashima, T., Fujiyama, T., Kawaguchi, Y., Nabeshima, Y. and Hoshino, M. (2007). Origin of climbing fiber neurons and their developmental dependence on Ptf1a. *J. Neurosci.* **27**, 10924-10934.
Yamasaki, T., Kawaji, K., Ono, K., Bito, H., Hirano, T., Osumi, N. and Kengaku, M. (2001). Pax6 regulates granule cell polarization during parallel fiber formation in the developing cerebellum. *Development* **128**, 3133-3144.
Yang, Q., Bermingham, N. A., Finegold, M. J. and Zoghbi, H. Y. (2001). Requirement of Math1 for secretory cell lineage commitment in the mouse intestine. *Science* **294**, 2155-2158.
Yoshizawa, M., Hoshino, M., Sone, M. and Nabeshima, Y. (2002). Expression of stef, an activator of Rac1, correlates with the stages of neuronal morphological development in the mouse brain. *Mech. Dev.* **113**, 65-68.
Yoshizawa, M., Sone, M., Matsuo, N., Nagase, T., Ohara, O., Nabeshima, Y. and Hoshino, M. (2003). Dynamic and coordinated expression profile of dbl-family guanine nucleotide exchange factors in the developing mouse brain. *Gene Expr. Patterns* **3**, 375-381.
Yoshizawa, M., Kawauchi, T., Sone, M., Nishimura, Y. V., Terao, M., Chihama, K., Nabeshima, Y. and Hoshino, M. (2005). Involvement of a Rac activator,P-Rex1, in neurotrophin-derived signaling and neuronal migration. *J. Neurosci.* **25**, 4406-4419.